Proceedings of the 21st ICSMGE, Vienna, Austria, 14 – 19 June 2026. Pistrol, Adam & Schweiger (eds.)
Published by: ÖGG, Austrian Society for Geomechanics, Salzburg, Austria, ISBN 978-3-9503898-4-5
https://doi.org/10.53243/ICSMGE2026-509

The role of water-temperature coupling effect on microstructure evolution of coal: Advanced insights from CT scanning and lab studies

Maleesha R.K.S., Kumari W. G. P., Jayan S. Vinod
School of Civil, Mining, Environmental and Architectural Engineering, University of Wollongong, NSW 2522, Australia, rksm899@uowmail.edu.au

ABSTRACT: Repurposing the underground voids and mine infrastructure left by abandoned mines for applications such as constructing energy reservoirs, including geothermal energy, thermal energy storage, compressed air energy storage, pumped hydro storage, flood control, and water storage, can enhance the efficiency of underground space usage. Despite its potential, the broad application of underground void spaces has been hindered by the limited understanding of the damage mechanisms of reservoir rocks, particularly under long-term water saturation, elevated temperature, pressure and gases. This study explores the microstructure evolution of coal under the coupled effects of water saturation and temperature at low temperatures (<60 °C). A series of comprehensive X-ray computed tomography (CT) experiments was conducted to analyse the microstructural changes and micro-cracking in coal samples subjected to two conditions: water saturation during heating and dry heating. All treated samples were scanned, reconstructed and subsequently, porosity was measured to identify total pore spaces The results revealed that total porosity and average pore size decreased with the increase of water-temperature and temperature. The findings of this study provide insights into how the coupled effect of water saturation and temperature affects the integrity of coal, which is a critical consideration for optimising the design and stability of underground energy storage systems and further contributing to the long-term safety and sustainability of mining operations.

Keywords: Temperature impact, CT scanning, coal, microstructure, cracks

1 INTRODUCTION

Globally, there are over a million abandoned mines, many of which present unique opportunities for alternative energy applications (Ai et al. 2021). Abandoned mines hold great potential for energy and space reuse. Repurposing them for geothermal energy, oil and gas storage, or other subsurface uses can greatly improve underground space efficiency. Among these, using flooded mines for geothermal energy recovery is a promising option. Over time, abandoned mines tend to fill with water from sources such as groundwater inflows, surface runoff, and old excavation water (Wang et al. 2022). This accumulated mine water, due to its relatively stable temperature and extensive subsurface network, can serve as an effective medium for low-enthalpy geothermal energy systems. Utilising mine water from flooded mines for geothermal applications not only supports renewable energy goals but also revitalises former mining regions both economically and environmentally.

However, once mines become flooded, the persistent presence of water induces substantial changes in the hydrogeological and thermal environment of the surrounding rock mass. Ongoing seepage through fracture zones exposes geological formations to coupled water–temperature effects, which alter both mechanical integrity and thermal behaviour. The presence of water in these subsurface environments not only contributes to the degradation of the mechanical properties of coal and rock but can also trigger various geotechnical hazards, such as coal pillar spalling, mine collapse, and tunnel deformation (Han et al. 2022). These evolving conditions pose significant risks to the long-term stability and functionality of repurposed mine workings. Therefore, a comprehensive understanding of the geomechanical response of coal and adjacent rock under such complex environmental influences is critical to ensuring the safe and sustainable reuse of underground mine infrastructure.

Previous studies have primarily investigated the effects of water on the mechanical behaviour of coal (Yao et al. 2020; Ai et al. 2021; Han et al. 2022). They have demonstrated that water infiltration leads to a significant reduction in the mechanical strength of coal and associated coal-measure rocks. In terms of acoustic emission (AE) behaviour, higher moisture content increases the concentration of internal energy, indicating more low-energy events, and the development of a more complex crack network (Han et al. 2022; Liu et al. 2020).

While many previous studies have focused on the macroscopic mechanical behaviour of coal under varying moisture conditions, less attention has been given to the underlying microstructural changes that govern these responses. Since macroscopic fractures often originate from the accumulation and propagation of microcracks, understanding how different degrees of water saturation influence microcrack development and the overall microstructure is essential. Researchers have employed various techniques, such as scanning electron microscopy (SEM) (Ai et al. 2021; Han et al. 2022), industrial computed tomography (CT) (Han et al. 2022), and mercury injections (Yao et al. 2019) to examine the microstructure of coal and rock. These methods have been instrumental in analysing pore geometry and fracture network within the material. Although previous work has been published on the effect of water and temperature separately, few studies have focused on the effect of the coupled water and temperature effect on the microstructure of coal. This study aims to address this gap by investigating the microstructural alterations in coal subjected to varying water temperatures.

2 WATER SATURATION AND THERMAL EFFECTS ON COAL MICROSTRUCTURE

2.1 *Water saturation effects*

Water saturation plays a critical role in altering the pore structure and fracture network within coal. The absorption of water, especially in coals containing hydrophilic clay minerals like illite, leads to matrix swelling and weakening of interparticle bonds, and the initiation of fractures along cleats and bedding planes. This enhances crack length, width, and connectivity. As shown in Figure 1, the cumulative pore volume increases notably after water intrusion, particularly in the 2-10 nm range, indicating new pore formation through mineral dissolution. Continued swelling deforms the coal skeleton, further increasing pore volume. Although the growth rate slows at larger pore sizes, overall pore number and volume rise significantly (Si et al. 2021). These changes promote the development of interconnected flow channels and enhance coal permeability.

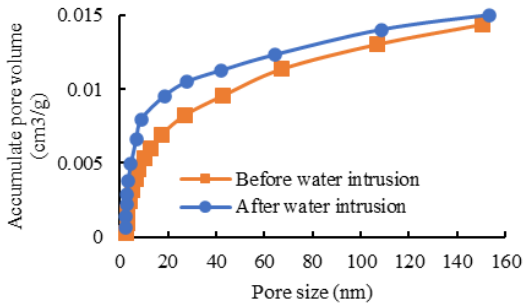

Figure 1. Accumulate pore volume of coal before and after water intrusion (adapted from (Si et al. 2021).

2.2 *Thermal effects*

Both microcracking and mineral expansion/decomposition contribute to thermal damage in rocks, leading to microstructural degradation. While the effect of mild temperatures (20 to 200 °C) on rock strength has been studied, results remain inconsistent due to variations in mineral composition and pore structures. Some studies report strength reduction with heating (Singh et al. 2015), while others observe minimal change or even strength gains (Kumari et al. 2017; Sirdesai et al. 2018). This variability reflects the complex thermo-mechanical response of rocks influenced by mineral composition, pore structure, and thermal expansion behaviours. In coal, thermal damage is more distinct: Below 100 °C, evaporation of free water and desorption of gas cause a reduction in average pore diameter, as fluid-filled spaces contract. Simultaneously, mineral expansion promotes matrix densification. However, above 100 °C, escalating thermal stress induces microcrack formation, gradually increasing pore connectivity and average pore size. Zhao et al. (2021) revealed that heating coal from 30 °C to 150 °C increased the total pore volume from 0.0419 to 0.0673 ml/g, (Figure 2) primarily due to macropore expansion, while mesopores, transition pores, and micropores showed minimal change.

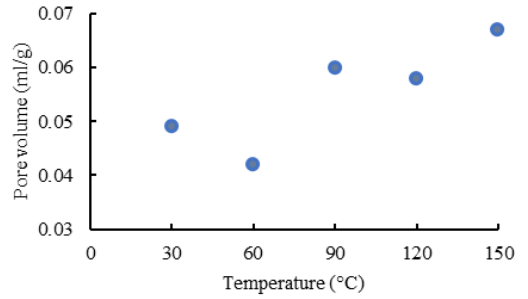

Figure 2. Accumulate pore volume of coal at different temperatures (adapted from (Zhao et al. 2021)).

3 MATERIALS AND METHODS

3.1 *Material properties and sample preparation*

In this study, the coal samples were obtained from a mine located in the Sydney Basin. Then coal samples were cut into small cubic specimens measuring approximately 10 mm (Figure 3). Sets of samples were then fully submerged in water and incubated under controlled temperature conditions of 40 °C and 60 °C for a duration of one month to simulate long-term thermal and saturation effects. Another set of samples was heated in an oven at 40 °C and 60 °C for two hours. After heating, these samples were allowed to cool naturally and then sealed in airtight bags for preservation. The corresponding proximate analysis data of coal samples are given in Table 1. This study assumed coal to be homogeneous, with pores and cracks evenly distributed.

Table 1. Proximate analysis of coal samples used in this study.

Inherent moisture (%)	Ash content (%)	Volatile content (%)	Fixed carbon content (%)
0.84	45.2	13.9	40.1

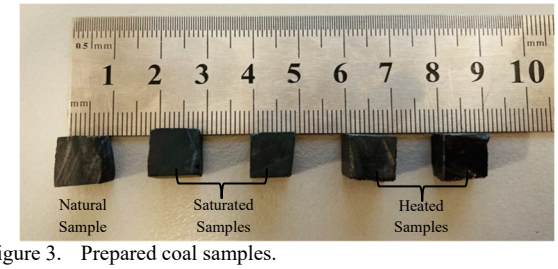

Figure 3. Prepared coal samples.

3.2 *Experimental procedure for micro-CT scanning*

Prepared samples were scanned using the micro-CT scanning facilities available in the Australian Synchrotron (Figure 4) to explore the microstructural characteristics of rock samples. Micro CT scanning equipment mainly consists of four components: (1) an X-ray source, (2) an X-ray detector, (3) a rotation stage and (4) a software system. In these experiments, a magnification of 1.8× was used, resulting in an effective pixel size of 3.611 µm.

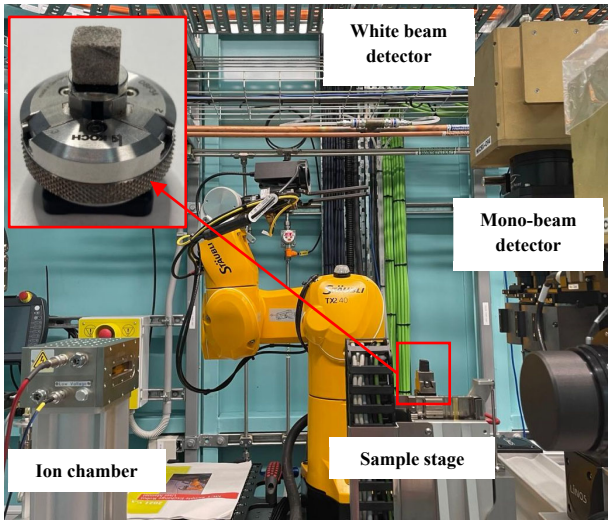

Figure 4. Optical table set-up at Australian Synchrotron MCT beamline.

X-ray attenuation through the material was interpreted using the Lambert–Beer law, where differences in grayscale intensity across the images correspond to variations in the material's internal density. The relationship between incident and transmitted X-ray intensities can be expressed as Equation (1) (An et al. 2022):

$$I = I_0 \exp(-\mu_m \chi \rho_i) \quad (1)$$

where I is the intensity after penetration (µm), I_0 is the intensity before penetration (µm), μ_m is absorption coefficient of unit weight (cm^2/g), χ is the penetration length of X-ray (cm), and ρ_i is the density of the corresponding mineral (g/cm^3) respectively. Finally, the obtained images were stitched and reconstructed in the Australian Synchrotron facility as a stack of two-dimensional cross-sectional images, enabling detailed three-dimensional visualisation and quantitative analysis of the internal structure.

3.3 *Numerical analysis procedure for porosity*

Image analysis was conducted using the FIJI software platform. A detailed procedure is depicted in Figure 5. A median filter was employed to suppress noise while preserving the structural integrity of the original features. Subsequently, unsharp masking was applied to the noise-removed images to enhance edge definition and facilitate the delineation of mineral boundaries. The differentiation of mineral phases was based on variations in grayscale intensity within the micro-CT images, which are influenced by the density and atomic number of the constituent materials. Minerals with lower densities appeared with higher grayscale values, whereas voids and fractures, exhibiting the highest X-ray attenuation contrast, were distinctly visualised as black regions in the reconstructed images. A thresholding technique was then applied to segment pore spaces from the solid matrix. A consistent thresholding method was applied across all micro-CT datasets, based on a standardised grayscale histogram analysis, ensuring uniform segmentation of pore and solid phases. The total pore area was obtained from the thresholded regions. The total sample area was measured by selecting the entire image. Porosity was then calculated using the Equation (2).

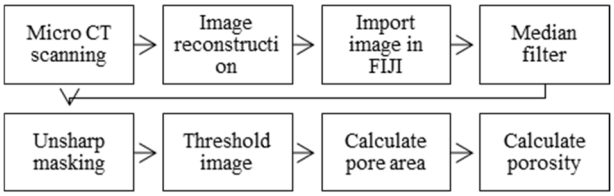

Figure 5. Procedure for porosity calculation.

$$Porosity = \left(\frac{Total\ pore\ area}{Total\ sample\ area}\right) \times 100\% \qquad (2)$$

4 RESULTS

2D images obtained for each sample using micro-CT were analysed through FIJI software following the procedure explained in Section 3.3. Figure 6 represents the 2D images of the raw sample and the total porosity of the natural sample. In total porosity images, red spots indicate the pores in the sample.

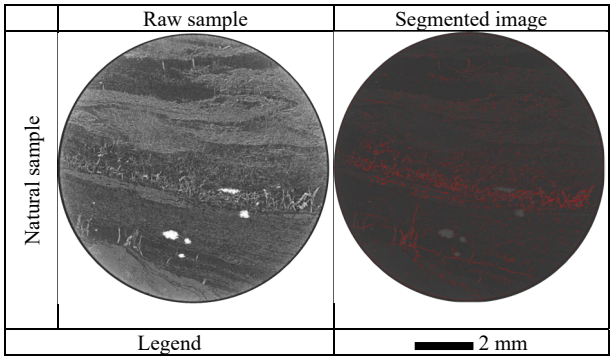

Figure 6. 2D image of raw sample and total porosity.

Total porosity was calculated using Eq. (2), and the corresponding results are summarised in Figure 7. The observed variation in porosity across different slices reflects intrinsic heterogeneity within the coal matrix, indicating spatially variable pore structures at the microscale. Average porosity was calculated across all slices to provide a summary measure of the sample's overall pore structure, as summarised in Table 2; however, given the observed slice-to-slice variability, this value should be interpreted alongside measures of dispersion to account for the inherent heterogeneity within the coal matrix. A significant reduction in average porosity was observed in the water-saturated samples, with a further decline noted as water temperature increased. For instance, the average total porosity of the natural coal sample, measured at 2.36%, decreased to 1.55% when saturated at 40 °C, and further declined to 1.33% when saturated at 60 °C. These results suggest a correlation between coal porosity variation, water saturation and water temperature. Similarly, in the heated samples, a progressive reduction in porosity was observed with rising temperature. The average total porosity decreased from 1.18% at 40 °C to 0.88% at 60 °C, indicating that thermal effects alone can also promote pore closure in coal.

The overall average pore sizes are also summarised in Table 2. A noticeable reduction in average pore size was also observed in the water-saturated samples, with a further decrease corresponding to elevated water temperatures. Progressive reduction in average pore size was observed in the heated samples, with smaller pores at higher temperatures.

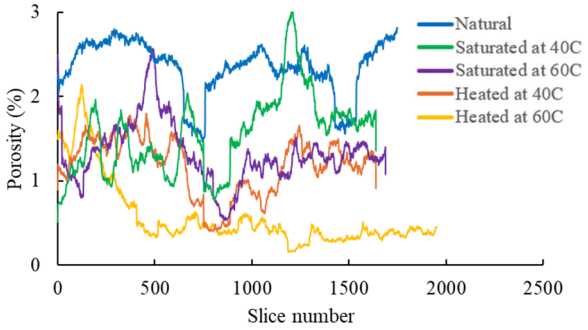

Figure 7. Variation of total porosity along slice number.

Table 2. Average total porosity and average pore sizes.

Condition	Average total porosity	Average pore size (μm)
Natural	2.36 %	78.97
Saturation while heating to 40 °C	1.55 %	62.07
Saturation while heating to 60 °C	1.33 %	59.68
Heated at 40 °C	1.18%	57.28
Heated at 60 °C	0.88%	57.08

5 DISCUSSION

These experimental results indicate that water saturation and an increase in water temperature/dry temperature can result in a decrease in porosity of the coal samples. Coal is composed of clay minerals and organic matter (such as vitrinite and inertinite), which can absorb water and swell. At moderate temperatures (40–60 °C), increased water mobility may enhance swelling of the organic matrix and expansion or softening of clay minerals, leading to the closure of existing pores and micro-cracks. As a result, both total and interconnected porosity are reduced. Jiang et al. (2024) also observed that increased water exposure led to widespread dispersion of clay mineral particles around coal pores and fissures. Higher water temperature (60 °C) could promote more swelling.

The effect of water temperature/ dry temperature on rock behaviour is likely driven by a main mechanism: the mechanical response from thermal expansion due to temperature changes (Heard, 1980). As water temperature/dry temperature rises, thermal expansion occurs along mineral grains, slightly increasing the rock's volume (Yang et al. 2019). This expansion generates internal thermal stress due to differences in the expansion rates and anisotropic behaviour of various minerals. In saturated coal, heating the water also contributes to internal thermal stress, but within the studied

range (40 °C and 60 °C), this stress remains well below the strength threshold of primary minerals like quartz and pyrite, so it does not cause new fracturing (Lu et al. 2017). However, thermal expansion can lead to coal matrix expansion, resulting closure of micro-pores and micro-cracks, reducing the rock's porosity. As illustrated in Figure 8, Zhao et al. (2021) and Shao et al. (2022) also reported a decrease in porosity with increasing temperature within a low temperature range (<100 ^{0}C), consistent with the present study.

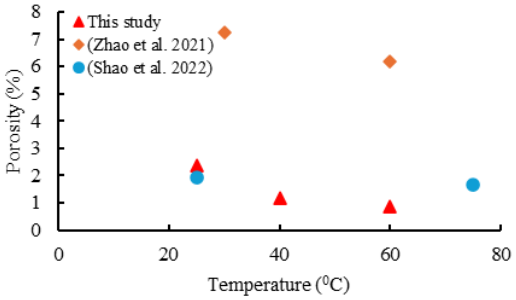

Figure 8. Variation of porosity with dry temperature

However, there are limitations on the method of CT image analysis. While CT scanning combined with reconstruction algorithms allows for quantitative comparison of pore structure and mineral composition before and after treatments, the method is sensitive to threshold selection during image segmentation and CT resolution limits. Additionally, the small sample size (approximately 10 mm cubes) poses limitations, as coal's inherent heterogeneity at micro to meso-scales (including cleats, fractures, and laminae) may not be fully represented. Local variations in microstructure, mineral content, and the orientation of natural fractures can introduce significant variability in measured porosity, even among samples taken from the same block. Micro-CT analysis provides pore-scale parameters such as geometry and connectivity, which can be upscaled using representative elementary volume analysis or homogenisation methods. These effective properties can then be incorporated into meso- and macro-scale thermal–fluid models, enabling prediction of larger-scale behaviour based on microstructural mechanisms.

6 CONCLUSIONS

Micro-CT technology was utilised to investigate the microstructural changes in coal resulting from water saturation and varying water temperatures. Subsequently, the FIJI software was employed to analyse total porosity and average pore size in the saturated coal samples. The conclusions of this study were drawn based on the insights gained from these analyses.

- Existing pores in the natural coal sample were visualised by utilising FIJI software.
- Both total porosity and average pore size were decreased with the increase in water temperature/dry temperature

These findings enhance the understanding of coal's microstructural behaviour under thermal and hydraulic influences, supporting the safe and sustainable reuse of underground mine infrastructure in geotechnical applications. This study represents preliminary work, and further research is needed to confirm the findings. Future work should include longer-term monitoring (up to 2–3 months) to assess potential delayed porosity increase from thermal cracking. Porosity changes should also be validated by supplementing CT analysis with mercury intrusion porosimetry (MIP) and scanning electron microscope (SEM). Additionally, detailed pore network and damage analysis are recommended to better understand microstructural evolution.

7 ACKNOWLEDGEMENTS

This work was supported by the Australian Research Council (ARC) under the Discovery Early Career Researcher Award (DECRA) scheme DE240100204. The authors acknowledge scientists at the Micro-CT facility at Australian Nuclear Science and Technology Organisation (ANSTO) for their assistance under project no. 23543. The authors also express their gratitude to the staff of the Geotechnical Engineering Laboratory at the University of Wollongong, Australia, for their support in conducting experiments.

8 REFERENCES

Ai, T. et al. 2021. Changes in the structure and mechanical properties of a typical coal induced by water immersion. *International Journal of Rock Mechanics and Mining Sciences* 138 104597.

An, R., Kong, L., Zhang, X. and Li, C. 2022. Effects of dry-wet cycles on three-dimensional pore structure and permeability characteristics of granite residual soil using X-ray micro computed tomography. *Journal of Rock Mechanics and Geotechnical Engineering* 14(3) 851-860.

Hall, A., Scott, J.A. and Shang, H. 2011. Geothermal energy recovery from underground mines. *Renewable and Sustainable Energy Reviews* 15(2) 916-924.

Han, P. et al. 2022. Effects of water on mechanical behavior and acoustic emission characteristics of coal in Brazilian tests. *Theoretical and Applied Fracture Mechanics* 122 103636.

Heard, H. 1980. Thermal expansion and inferred permeability of climax quartz monzonite to 300 C and 27.6 MPa. International Journal of Rock Mechanics and Mining Sciences & Geomechanics Abstracts, Elsevier.

Jiang, T. et al. 2024. Deterioration evolution mechanism and damage constitutive model improvement of sandstone–coal composite samples under the effect of repeated immersion. *Physics of Fluids* 36(5).

Kumari, W. et al. 2017. Mechanical behaviour of Australian Strathbogie granite under in-situ stress and temperature conditions: An application to geothermal energy extraction. *Geothermics* 65 44-59.

Liu, Y. et al. 2020. Mechanical properties and failure behaviour of dry and water-saturated anisotropic coal under true-triaxial loading conditions. *Rock Mechanics and Rock Engineering* 1-20.

Lu, Y., Wang, L., Sun, X. & Wang, J. 2017. Experimental study of the influence of water and temperature on the mechanical behaviour of mudstone and sandstone. *Bulletin of Engineering Geology and the Environment*, 76, 645-660.

Shao, H., Yang, S. & Yang, K. 2022. Effect of thermal damage on pore development and oxidation reaction of coal. *Asia-Pacific Journal of Chemical Engineerng,* 17, e2774

Si, L. et al. 2021. The influence of long-time water intrusion on the mineral and pore structure of coal. *Fuel* 290 119848.

Singh, B. et al. 2015. Thermo-mechanical properties of Bundelkhand granite near Jhansi, India. *Geomechanics and Geophysics for Geo-Energy and Geo-Resources* 1(1) 35-53.

Sirdesai, N., Gupta, T., Singh, T. and Ranjith, P. 2018. Studying the acoustic emission response of an Indian monumental sandstone under varying temperatures and strains. *Construction and Building Materials* 168 346-361.

Wang, K. et al. 2022. Experimental study on dynamic mechanical characteristics and fracture behaviours of coal under water–gas-temperature coupling conditions. *Theoretical and Applied Fracture Mechanics* 122 103609.

Yang, Y. et al. 2019. Experimental study on pore-fracture evolution law in the thermal damage process of coal. *International Journal of Rock Mechanics and Mining Sciences* 116 13-24.

Yao, Q. et al. 2019. Influence of moisture on crack propagation in coal and its failure modes. *Engineering Geology* 258 105156.

Yao, Q. et al. 2020. Experimental investigation of the mechanical failure behaviour of coal specimens with water intrusion. *Frontiers in Earth Science* 7 348.

Zhao, S. et al. 2021. Experimental analysis of the effect of temperature on coal pore structure transformation. *Fuel* 305 121613.